Modified Discrete-Time Super-Twisting Control of PMSM Speed Regulation System: Theory and Experimentation

Keqi Mei, *Member, IEEE*, Qiyue Li, Weile Chen, Chih-Chiang Chen, *Senior Member, IEEE*, and Shihong Ding, *Senior Member, IEEE*

***Abstract*—The article puts forward a modified discrete-time super-twisting (DTST) control strategy for the speed regulation system of permanent magnet synchronous motor (PMSM) to strengthen the control efficacy and resilience to disturbances in its digital execution. As opposed to the conventional DTST algorithm, the most discernible attribute for the developed scheme is to displace the discontinuous term in the conventional DTST by dint of a nonsmooth term in consequence of the constraint of the sampling frequency practically speaking. With consideration for this substitution, a flexibly tunable fractional power parameter is introduced to increase the control precision while mitigating the oscillations. The Lyapunov-based theoretical analysis is offered to rigorously validate the convergence for the correspondingly whole system. Eventually, in comparison with two existing control schemes, the effectiveness and superiority of the presented method are experimentally supported in real time through using a 1.5 kW PMSM hardware platform.**

***Index Terms*—Digital control, permanent magnet synchronous motor (PMSM), speed regulation, super-twisting algorithm.**

I. Introduction

CURRENTLY, among a vast array of alternating current electric machine drives, the permanent magnet synchronous motor (PMSM) has garnered significant focus domestically and internationally, as documented in [1], [2], and [3]. The reasons behind its popularity lie in its beneficial characteristics involving high power density, low noise, compact structure, wide speed range, friendly maintenance, and high efficiency [4]. As such, the PMSM has been in the broad use across diverse industrial plants, e.g., power generations, robots, and aircrafts [5].

Notwithstanding its multiple merits described earlier, it is exceedingly arduous to realize the high-accuracy speed regulation of PMSM under multifarious operational settings through exclusively utilizing linear control approaches (e.g., proportional-integral controllers). The explanation is that the motion dynamics of PMSM are intrinsically time-varying, nonlinear, and coupled. Meanwhile, numerous real factors, such as unmodeled dynamics, parameter variations, friction torques, and external disturbances, unavoidably incur obstacles in fulfilling this target [6]. How to alleviate these detrimental impacts in the speed regulation system of PMSM is accordingly one of the pivotal matters that deserves to be deeply pondered by practitioners. Over the past few decades, substantial research endeavors have been made to introduce a range of advanced nonlinear control strategies into the PMSM speed regulation system, such as iterative learning control [7], adaptive control [8], fuzzy control [9], just to list a few.

As a frequently employed nonlinear control approach, the sliding mode control (SMC) has been demonstrated to be a compelling method in terms of efficiently handling the disturbances and promptly reacting to the given system requirements. The fact renders the SMC to become a preferable alternative for tackling the problem of the PMSM speed regulation in face of probable various sources of disturbances. In [10], a composite SMC strategy was reported to strengthen the ability against disturbances for the PMSM speed regulation system. Nonetheless, the system convergence time to zero under such a conventional first-order SMC (FOSMC) framework is infinite. This does not necessarily meet the practical application demand of the high performance speed regulation of PMSM. One potential solution to surmount the aforesaid trouble through bringing in a nonlinear component to the linear sliding manifold is the terminal SMC (TSMC) [11]. Grounded on this TSMC method, the speed regulation issue of PMSM was explored in [12] to fulfill the finite-time convergence to zero. In an attempt to further accelerate the dynamic response time of PMSM, a nonsingular fast TSMC scheme was provided in [13].

Nonetheless, a conspicuous drawback for the above traditional SMC approaches applied in PMSM is the inherent chattering appearance stemming from the discontinuous switching

Received 13 September 2024; revised 26 December 2024; accepted 9 February 2025. Date of publication 13 February 2025; date of current version 20 March 2025. This work was supported in part by the National Natural Science Foundation of China under Grant 62203188 and Grant 62373170, in part by the National Key Research and Development Program of China under Grant 2022YFD200150203, in part by the Natural Science Foundation of Jiangsu Province under Grant BK20220517, in part by the China Postdoctoral Science Foundation under Grant 2022M721386, and in part by the National Science and Technology Council (NSTC), Taiwan, under Grant NSTC 113-2221-E-006-145-MY2. Recommended for publication by Associate Editor R. Kennel. *(Corresponding author: Chih-Chiang Chen.)*

Keqi Mei, Qiyue Li, and Shihong Ding are with the School of Electrical and Information Engineering, Jiangsu University, Zhenjiang 212013, China (e-mail: mkq@ujs.edu.cn; 2222207047@stmail.ujs.edu.cn; dsh@ujs.edu.cn).

Weile Chen is with the School of Automation, Southeast University, Nanjing 210096, China (e-mail: weilechen@seu.edu.cn).

Chih-Chiang Chen is with the Department of Systems and Naval Mechatronic Engineering, National Cheng Kung University, Tainan 70101, Taiwan (e-mail: ccchenevan@ncku.edu.tw).

Color versions of one or more figures in this article are available at https://doi.org/10.1109/TPEL.2025.3541340.

Digital Object Identifier 10.1109/TPEL.2025.3541340

behavior of the control law as the system states traverse the sliding manifold. Such an unfavorable impact will ultimately impair the PMSM mechanical components, waste the energy and diminish the control efficiency. With the aim of relieving the phenomenon, there have been various control strategies documented in the literature [14], [15], [16]. Among them, the boundary layer based method put forward in [17] is widely used by taking the place of the switching term with an approximated function. Regrettably, this method will dramatically undermine the system robustness and generate the steady-state errors. Another promising control strategy is the second-order sliding mode (SOSM) suggested by [18]. The basic principle behind the SOSM framework is to incorporate the discontinuous switching term to attain the control input while retaining the excellent properties of the traditional FOSMC. With respect to observation and robust control, one of the most prevalent SOSM methods is the super-twisting algorithm (STA) on account of the three points. First, the strong antijamming capability and the finite-time convergence of systems under consideration can be attained under the STA [19]. Second, solely the information regarding the sliding variable is demanded to be accessible in the STA [20]. At last, the STA possesses the ability to efficaciously mitigate the inevitable chattering in conventional FOSMC dynamics [21]. The three virtues stimulate its successful application to the PMSM system [22], [23], [24], [25]. In [22], the authors designed a composite STA to address the PMSM speed regulation issue. Through taking into account the negative effect of inertia fluctuations, a super-twisting SMC scheme was proposed for a PMSM drive system with an inertia identification in [25]. Nonetheless, it must be noted that all foregoing SMC strategies used for PMSM systems are constructed from the continuous-time perspective.

Since the practically widespread implementation of controllers hinges on digital computers, there has recently been an escalating attention on the design of diverse discrete-time sliding mode (DTSM) controllers. It should be emphasized that theoretically, the attributes applicable to continuous-time SMC can not be directly expanded into its discrete-time counterpart as a result of the immanent finite sampling frequency of digital processors. In general, the ideas of designing these DTSM for the considered systems are categorized into two types. One is designated as the emulation approach, in which the DTSM controllers are acquired through discretizing the continuous-time sliding mode controllers. In line with the thought, several outcomes have been reported in [26], [27], and [28]. Nevertheless, if the control action can not be carried out promptly, it is quite arduous to accomplish the expectant aim via this method. The other is called as the redesigned strategy, where the continuous-time system is first discretized and then the intended controller is constructed for the derived discrete-time system. Within this scheme, the DTSM controllers mainly contain the reaching law-based DTSM controllers [29], [30], [31] and the equivalent control based DTSM controllers [32], [33], [34]. More recently, the DTSM control methods have been extensively adopted in PMSM systems [35], [36].

It is noteworthy that all the previously mentioned discrete-time SMC strategies are put forward on the basis of FOSMC schemes. Spurred by these studies, the discrete-time SOSM control approaches have been recently presented [37], [38], [39], [40]. In [38], the authors introduced the discrete-time variants of STA via an eigenvalue-based conversion. In [39], the implicit discretization of STA was analyzed and discussed. Since this method in [39] needs more intricate computational requirements, the explicit Euler's discretization effect on the STA was studied in [40] by utilizing the geometric approach. However, these discrete-time super-twisting (DTST) control strategies encompass the discontinuous switching term, resulting in the occurrence of the chattering and the reduction of the control precision. If these DTST control strategies are applied to the PMSM system, then the chattering will cause the output speed fluctuation during the real-time execution. Besides, the discontinuous switching term is significantly impacted by the limited sampling frequency of the PMSM system, thereby leading to great challenges in practical implementation. Up to now, how to devise a modified DTST control approach for the PMSM speed regulation system that can mitigate the speed fluctuation and improve the control accuracy is still an open research issue.

Encouraged by the foregoing observations and discussions, our work endeavors to develop a modified DTST control framework for the PMSM speed regulation system under the restricted sampling frequency. In comparison with the current results, the significant contributions in the article are underscored as follows.

1) A modified DTST control law is developed for the PMSM speed regulation system via the introduction of an additional parameter to make the discontinuous switching term in the traditional DTST algorithm turn into a nonsmooth term. This manipulation can alleviate the effect of the sampling frequency on the digital implementation of the PMSM speed regulation system.
2) Under the proposed control scheme, the tracking error between the actual speed and its desirable value can finite-time converge to an ultimate bound with rejecting the disturbances. The rigorous theoretical analysis is performed to analyze and discuss the impacts of the sampling period and the disturbance on the control accuracy of the presented method. Compared with the conventional DTST approach reported in [38], [39], and [40], the proposed algorithm possesses the higher output tracking accuracy.
3) The comparative results acquired through real-time experimental tests for the PMSM speed regulation system are provided to clearly illustrate the efficiency and merits of the suggested control scheme.

The rest of this article is organized as follows. Section II gives the modeling of PMSM and problem characterization. The method of designing the modified DTST controller for PMSM is offered in Section III, where the corresponding stability analysis is also elaborated. Section IV shows and discusses the real-time comparative experiment results on the PMSM speed regulation system. Finally, Section V concludes this article.

Notations: $\mathbb{R}$ denotes the set of real numbers, and $\mathbb{N}^+$ represents the set of nonnegative integers. For all $\xi, \vartheta \in \mathbb{R}$, $\lceil \xi \rfloor^{\vartheta} = |\xi|^{\vartheta} \cdot \mathrm{sign}(\xi)$, where $\mathrm{sign}(\cdot)$ is the sign function. The notation $O(\cdot)$ signifies that a function $F(s) : \mathbb{R} \to \mathbb{R}$ is

perceived as of order $G(s):\mathbb{R}\to\mathbb{R}$ when $s\to 0$ and represented as $F(s)=O(G(s))$, if there exist real numbers $\vartheta_1,\vartheta_2>0$ such that $|F(s)|<\vartheta_1|G(s)|$ for $|s|<\vartheta_2$.

II. System Modeling and Problem Formulation

Through following the work introduced by [41], one can characterize the motion equation of PMSM system as

$$\dot{\omega}(t)=-\frac{B}{J}\omega(t)-\frac{T_L}{J}+\frac{K_t}{J}i_q=-\frac{T_d}{J}+\frac{K_t}{J}i_q^* \tag{1}$$

where $\omega(t)$ is the angular velocity, B is the viscous coefficient, J is the moment of inertia, T_L is the load torque, K_t is the torque constant, i_q is the stator current of q axis, i_q^* is the reference current of q axis, and $T_d=T_L+B\omega(t)+K_t(i_q^*-i_q)$ is the lumped disturbance torque.

By defining the desired angular velocity as ω^*, one yields the tracking error as

$$e(t)=\omega(t)-\omega^*. \tag{2}$$

It follows from (1) and (2) that:

$$\dot{e}(t)=u(t)+D(t) \tag{3}$$

where $u(t)=\frac{K_t}{J}i_q^*$ and $D(t)=-\frac{T_d}{J}-\dot{\omega}^*$, which satisfies

Assumption 1: The lumped perturbation $D(t)$ is piecewise, i.e., $D(t)=D(t_k)$ for $t\in[t_k,t_{k+1})$, where t_k, t_{k+1} are the sampling points, $k\in\mathbb{N}^+$, $t_{k+1}=t_k+T$, $T>0$ is the sampling period. Moreover, the change rate of $D(t_k)$ is bounded, i.e., $\sup|\frac{D(t_{k+1})-D(t_k)}{T}|\le D^*$ with one positive constant D^*.

On the basis of the model (3), the control goal is to construct an appropriate control scheme, such that the tracking errors are steered to zero. Although several results on constructing such a controller for the PMSM speed regulation system by utilizing SOSM strategies, e.g., see [4], [22], [42], [43], these control schemes are essentially established on the continuous-time SOSM theory. Distinct from these consequences, it is assumed in the paper that the control signal $u(t)$ is digitally implemented via a zero-order hold, i.e., $u(t)=u(t_k)$ over the time interval $[t_k,t_{k+1})$. To put it differently, the major aim of the article is to construct a discrete-time SOSM control law for the PMSM speed regulation system, which is more suitable for execution in a digital format.

To realize this objective, we first utilize the Euler discretization approach to obtain the corresponding discrete-time model of system (3), which is described as

$$e(t_{k+1})=(u(t_k)+D(t_k))\cdot T+e(t_k). \tag{4}$$

Based upon the discrete-time model, a discrete-time version of the super-twisting control law is given as [38] and [40]

$$\begin{cases}u(t_k)=-k_1\lceil e(t_k)\rfloor^{\frac{1}{2}}+v(t_k)\\ v(t_{k+1})=v(t_k)-k_2\cdot\mathrm{sign}(e(t_k))T\end{cases} \tag{5}$$

where k_1, k_2 are positive control parameters, and v is the state variable.

Substituting (5) into (4) gets

$$\begin{cases}x_1(t_{k+1})=x_1(t_k)+k_1\left(x_2(t_k)-\lceil x_1(t_k)\rfloor^{\frac{1}{2}}\right)T\\ x_2(t_{k+1})=x_2(t_k)-\frac{k_2}{k_1}\cdot\left(\mathrm{sign}(x_1(t_k))+d(t_k)\right)T\end{cases} \tag{6}$$

where $x_1(t_k)=e(t_k)$, $x_2(t_k)=\frac{v(t_k)+D(t_k)}{k_1}$ and $d(t_k)=\frac{D(t_k)-D(t_{k+1})}{k_2T}$.

The previous studies (e.g., see [38], [40]) have demonstrated that the state variables $x_1(t_k)$ and $x_2(t_k)$ of the whole system (6) ultimately converge to a bounded region in a neighborhood of the origin given by $\Omega_1=\{x_1,x_2\in\mathbb{R}:|x_1|\le\gamma_1T^2,\ |x_2|\le\gamma_2T\}$ with positive constants γ_1 and γ_2. In other words, the tracking error $e(t_k)$ has an accuracy level with $O(T^2)$. In addition, the periodic behavior (i.e., the discretization chattering) also eventually exists in system (6), since the discontinuous term $\frac{k_2T}{k_1}\cdot\mathrm{sign}(x_1(t_k))$ is embraced in system (6). This phenomenon will negatively impact the control performance and precision. Moreover, in real-world scenarios, the discontinuous term experiences substantial influence from the sampling time, leading to considerable challenges during its execution.

Stimulated by this observation, in the subsequent section, we will modify the standard DTST controller (5) so as to lessen the chattering effect and enhance the control precision.

III. Modified DTST Control Design for PMSM

With the intention of eliminating the discontinuous switching term in (5), by supplementing one parameter, a revamped DTST controller is constructed as

$$\begin{cases}u(t_k)=-k_1\lceil e(t_k)\rfloor^{1+\rho}+v(t_k)\\ v(t_{k+1})=v(t_k)-k_2\cdot\lceil e(t_k)\rfloor^{1+2\rho}T\end{cases} \tag{7}$$

where k_1 and k_2 are proper positive constants, and ρ is one constant satisfying $-\frac{1}{2}<\rho<0$.

Theorem 1: For system (4) under Assumption 1, if the control law is constructed as (7), then the system output $e(t_k)$ will finite-time converge to the domain

$$\Pi=\left\{e(t_k):|e(t_k)|\le\max\left\{\left(\frac{D^*}{k_2}\right)^{\frac{1}{1+2\rho}}\sigma_1,\ T^{-\frac{1}{\rho}}\sigma_2\right\}\right\} \tag{8}$$

where σ_1 and σ_2 are appropriate positive constants.

Proof: Substituting (7) into (4) produces

$$\begin{cases}x_1(t_{k+1})=x_1(t_k)+k_1\left(x_2(t_k)-\lceil x_1(t_k)\rfloor^{1+\rho}\right)T\\ x_2(t_{k+1})=x_2(t_k)-\frac{k_2}{k_1}\cdot\left(\lceil x_1(t_k)\rfloor^{1+2\rho}+d(t_k)\right)T\end{cases} \tag{9}$$

where $x_1(t_k)=e(t_k)$, $x_2(t_k)=\frac{v(t_k)+D(t_k)}{k_1}$ and $d(t_k)=\frac{D(t_k)-D(t_{k+1})}{k_2T}$. Evidently, from Assumption 1, one yields $|d(t_k)|\le\frac{D^*}{k_2}$.

Subsequently, we will analyze the stability of system (9).

First, for the analytical convenience, system (9) is rewritten as the following equivalent form:

$$\begin{cases}\dot{x}_1(t)=k_1\left(x_2(t_k)-\lceil x_1(t_k)\rfloor^{1+\rho}\right)\\ \dot{x}_2(t)=-\frac{k_2}{k_1}\cdot\left(\lceil x_1(t_k)\rfloor^{1+2\rho}+d(t_k)\right)\end{cases} \tag{10}$$

for $\forall t \in [t_k, t_{k+1})$. Furthermore, system (10) can be reworded as

$$\begin{cases} \dot{x}_1(t) = k_1 \left(x_2(t) - \lceil x_1(t) \rceil^{1+\rho} \right) + \eta_1 + \eta_3 \\ \dot{x}_2(t) = -\frac{k_2}{k_1} \cdot \left(\lceil x_1(t) \rceil^{1+2\rho} + d(t_k) \right) + \eta_2 \end{cases} \tag{11}$$

where $\eta_1 = k_1(\lceil x_1(t) \rceil^{1+\rho} - \lceil x_1(t_k) \rceil^{1+\rho})$, $\eta_2 = \frac{k_2}{k_1}(\lceil x_1(t) \rceil^{1+2\rho} - \lceil x_1(t_k) \rceil^{1+2\rho})$ and $\eta_3 = -k_1(x_2(t) - x_2(t_k))$.

Inspired by the work in [44], we consider the following Lyapunov function:

$$W = W_1 + W_2 \tag{12}$$

where $W_1 = (1+\rho)(1+\alpha_1)|x_2(t)|^{\frac{2}{1+\rho}}$ with one positive constant α_1 and $W_2 = \frac{1}{2}(x_1(t) - \lceil x_2(t) \rceil^{\frac{1}{1+\rho}})^2$.

For ease of facilitating the proof, the next proposition is offered, whose proof is analogous to that of Theorem 3.1 in [45], and hence is neglected for brevity.

Proposition 1: Along the following system:

$$\begin{cases} \dot{x}_1(t) = k_1 \left(x_2(t) - \lceil x_1(t) \rceil^{1+\rho} \right) \\ \dot{x}_2(t) = -\frac{k_2}{k_1} \cdot \left(\lceil x_1(t) \rceil^{1+2\rho} + d(t_k) \right) \end{cases} \tag{13}$$

differentiating W in (12) obtains $\dot{W}|_{(13)} \le -\frac{k_2}{2k_1}(|\xi|^{\frac{2+\rho}{1+\rho}} + |x_2|^{\frac{2+\rho}{1+\rho}}) + \frac{k_2}{k_1}\alpha_6(\frac{D^*}{k_2})^{\frac{2+\rho}{1+2\rho}}$, where α_6 is one positive constant and $\xi = \lceil x_1 \rceil^{1+\rho} - x_2$.

From Proposition 1, the time derivative of W in (12) along system (11) is

$$\begin{aligned} \dot{W}|_{(11)} \le & -\frac{k_2}{2k_1}\left(|\xi|^{\frac{2+\rho}{1+\rho}} + |x_2|^{\frac{2+\rho}{1+\rho}} \right) + \frac{k_2}{k_1}\alpha_6 \left(\frac{D^*}{k_2} \right)^{\frac{2+\rho}{1+2\rho}} \\ & + \frac{\partial W}{\partial x_1}\eta_1 + \frac{\partial W}{\partial x_1}\eta_3 + \frac{\partial W}{\partial x_2}\eta_2. \end{aligned} \tag{14}$$

In what follows, we will, respectively, estimate $\frac{\partial W}{\partial x_1}$ and $\frac{\partial W}{\partial x_2}$ in (14). It is derived from Lemma 1 that

$$\frac{\partial W}{\partial x_1} \le \alpha_8 \left(|\xi|^{\frac{1}{1+\rho}} + |x_2|^{\frac{1}{1+\rho}} \right) \tag{15}$$

with $\alpha_8 = 1 + 2^{\frac{-\rho}{1+\rho}}$. Then, through using Lemmas 1–2, one yields

$$\frac{\partial W}{\partial x_2} \le \alpha_9 \left(|\xi|^{\frac{1-\rho}{1+\rho}} + |x_2|^{\frac{1-\rho}{1+\rho}} \right) \tag{16}$$

where $\alpha_9 = 2 + 2\alpha_1 + \frac{1-2\rho+2^{\frac{-2\rho}{1+\rho}}}{1-\rho^2}$.

From Lemma 3, η_1 and η_2 in (14), respectively, satisfy

$$\eta_1 \le 2^{-\rho} k_1 |x_1(t) - x_1(t_k)|^{1+\rho}, \tag{17}$$

$$\eta_2 \le 2^{-2\rho} \frac{k_2}{k_1} |x_1(t) - x_1(t_k)|^{1+2\rho}. \tag{18}$$

Note that

$$|x_1(t) - x_1(t_k)| = \left| \int_{t_k}^{t} \dot{x}_1(t)dt \right| \le \int_{t_k}^{t} |\dot{x}_1(t)|dt, \tag{19}$$

$$|x_2(t) - x_2(t_k)| = \left| \int_{t_k}^{t} \dot{x}_2(t)dt \right| \le \int_{t_k}^{t} |\dot{x}_2(t)|dt. \tag{20}$$

Based upon (10), one obtains

$$\begin{cases} |\dot{x}_1(t)| \le k_1 |x_2(t_k)| + k_1 |x_1(t_k)|^{1+\rho} \\ |\dot{x}_2(t)| \le \frac{k_2}{k_1} |x_1(t_k)|^{1+2\rho} + \frac{D^*}{k_1} \end{cases}. \tag{21}$$

It is acquired from (12) that

$$|x_2| \le \alpha_{10} W^{\frac{1+\rho}{2}}, \ |x_1| \le \alpha_{11} W^{\frac{1}{2}} \tag{22}$$

where $\alpha_{10} = (\frac{1}{(\alpha_1+1)(\rho+1)})^{\frac{1+\rho}{2}}$ and $\alpha_{11} = \alpha_{10}^{\frac{1}{1+\rho}} + 2^{\frac{1}{2}}$.

As per Lemma 1, incorporating (19)–(22) produces

$$\begin{cases} |x_1(t) - x_1(t_k)| \le T\alpha_{12} W_{\max}^{\frac{1+\rho}{2}} \\ |x_2(t) - x_2(t_k)|^{\frac{2+\rho}{1+\rho}} \le \alpha_{13} T^{\frac{2+\rho}{1+\rho}} W_{\max}^{\frac{(1+2\rho)(2+\rho)}{2(1+\rho)}} \\ \qquad + \alpha_{14} T^{\frac{2+\rho}{1+\rho}} \left(\frac{D^*}{k_2} \right)^{\frac{2+\rho}{1+\rho}} \end{cases} \tag{23}$$

where $\alpha_{12} = k_1(\alpha_{10} + \alpha_{11}^{1+\rho})$, $W_{\max} = \max_{\delta \in [t_k, t]} W(\delta)$, $\alpha_{13} = 2^{\frac{1}{1+\rho}}(\frac{\alpha_{11}^{1+2\rho} k_2}{k_1})^{\frac{2+\rho}{1+\rho}}$, and $\alpha_{14} = 2^{\frac{1}{1+\rho}}(\frac{k_2}{k_1})^{\frac{2+\rho}{1+\rho}} < \alpha_{13}$.

Via Lemma 2, integrating (15), (17), and (23) attains

$$\frac{\partial W}{\partial x_1}\eta_1 \le \frac{k_2}{8k_1}\left(|x_2|^{\frac{2+\rho}{1+\rho}} + |\xi|^{\frac{2+\rho}{1+\rho}} \right) + \frac{k_2}{k_1}\alpha_{15} T^{2+\rho} W_{\max}^{\frac{(1+\rho)(2+\rho)}{2}} \tag{24}$$

with α_{15} being a positive constant.

Then, in light of Lemma 2, combining (16), (18), and (23) has

$$\frac{\partial W}{\partial x_2}\eta_2 \le \frac{k_2}{8k_1}\left(|x_2|^{\frac{2+\rho}{1+\rho}} + |\xi|^{\frac{2+\rho}{1+\rho}} \right) + \frac{k_2}{k_1}\alpha_{16} T^{2+\rho} W_{\max}^{\frac{(1+\rho)(2+\rho)}{2}} \tag{25}$$

where α_{16} is a positive constant.

Next, according to Lemma 2, it is acquired from (15) and (23) that

$$\begin{aligned} \frac{\partial W}{\partial x_1}\eta_3 \le & \frac{k_2}{8k_1}\left(|x_2|^{\frac{2+\rho}{1+\rho}} + |\xi|^{\frac{2+\rho}{1+\rho}} \right) + \alpha_{18}\frac{k_2}{k_1} T^{\frac{2+\rho}{1+\rho}} \left(\frac{D^*}{k_2} \right)^{\frac{2+\rho}{1+\rho}} \\ & + \alpha_{17}\frac{k_2}{k_1} T^{\frac{2+\rho}{1+\rho}} W_{\max}^{\frac{(1+2\rho)(2+\rho)}{2(1+\rho)}} \end{aligned} \tag{26}$$

where $\alpha_{17} = \alpha_{13}\frac{2\alpha_8 k_1^2(1+\rho)}{k_2(2+\rho)}(\frac{8\alpha_8 k_1^2}{(2+\rho)k_2})^{\frac{1}{1+\rho}}$ and $\alpha_{18} = \alpha_{14}\frac{2\alpha_8 k_1^2(1+\rho)}{k_2(2+\rho)}(\frac{8\alpha_8 k_1^2}{(2+\rho)k_2})^{\frac{1}{1+\rho}} < \alpha_{17}$.

Further, it follows from the definition of W in (12) and Lemma 1 that

$$W \le \alpha_7 \left(|x_2|^{\frac{2}{1+\rho}} + |\xi|^{\frac{2}{1+\rho}} \right) \tag{27}$$

where $\alpha_7 = 1 + (1+\rho)(1+\alpha_1) + 2^{\frac{1-\rho}{1+\rho}}$.

Substituting (24)–(27) into (14) produces

$$\begin{aligned} \dot{W}|_{(11)} \le & -\frac{k_2}{8k_1}\left(\frac{W}{\alpha_7} \right)^{\frac{2+\rho}{2}} + \frac{k_2}{k_1}\alpha_6 \left(\frac{D^*}{k_2} \right)^{\frac{2+\rho}{1+2\rho}} \\ & + \frac{k_2}{k_1}\alpha_{19} T^{2+\rho} W_{\max}^{\frac{(1+\rho)(2+\rho)}{2}} + \alpha_{18}\frac{k_2}{k_1} T^{\frac{2+\rho}{1+\rho}} \left(\frac{D^*}{k_2} \right)^{\frac{2+\rho}{1+\rho}} \\ & + \alpha_{17}\frac{k_2}{k_1} T^{\frac{2+\rho}{1+\rho}} W_{\max}^{\frac{(1+2\rho)(2+\rho)}{2(1+\rho)}} \end{aligned} \tag{28}$$

with $\alpha_{19} = \alpha_{15} + \alpha_{16}$.

Define the following domain:

$$\Psi=\left\{(x_1,x_2):W\leq\max\left\{\alpha_{21}T^{\frac{-2}{\rho}},\alpha_{20}\left(\frac{D^*}{k_2}\right)^{\frac{2}{1+2\rho}}\right\}\right\} \tag{29}$$

where $\alpha_{20}=\max\{1,\alpha_7(48\alpha_6)^{\frac{2}{2+\rho}}\}$ and $\alpha_{21}=\max\{(48\alpha_{19}\alpha_7^{\frac{2+\rho}{2}})^{\frac{-2}{\rho(2+\rho)}},(48\alpha_{17}\alpha_7^{\frac{2+\rho}{2}})^{\frac{-2(1+\rho)}{\rho(2+\rho)}}\}$.

Subsequently, we will prove that the system states finite-time converge to the domain Ψ in (29).

First, it is assumed that $(x_1,x_2)\notin\Psi$, which signifies that

$$W>\alpha_{21}T^{\frac{-2}{\rho}},\ W>\alpha_{20}\left(\frac{D^*}{k_2}\right)^{\frac{2}{1+2\rho}}. \tag{30}$$

By integrating $\alpha_{18}<\alpha_{17}$ and (30), one has

$$\begin{cases}\frac{k_2}{k_1}\alpha_6\left(\frac{D^*}{k_2}\right)^{\frac{2+\rho}{1+2\rho}}<\frac{k_2}{48k_1}\left(\frac{W}{\alpha_7}\right)^{\frac{2+\rho}{2}}\\ \frac{k_2}{k_1}\alpha_{19}T^{2+\rho}W^{\frac{(1+\rho)(2+\rho)}{2}}<\frac{k_2}{48k_1}\left(\frac{W}{\alpha_7}\right)^{\frac{2+\rho}{2}}\\ \frac{k_2}{k_1}\alpha_{17}T^{\frac{2+\rho}{1+\rho}}W^{\frac{(1+2\rho)(2+\rho)}{2(1+\rho)}}<\frac{k_2}{48k_1}\left(\frac{W}{\alpha_7}\right)^{\frac{2+\rho}{2}}\\ \alpha_{18}\frac{k_2}{k_1}T^{\frac{2+\rho}{1+\rho}}\left(\frac{D^*}{k_2}\right)^{\frac{2+\rho}{1+\rho}}<\frac{k_2}{k_1}\alpha_{17}T^{\frac{2+\rho}{1+\rho}}W^{\frac{(1+2\rho)(2+\rho)}{2(1+\rho)}}\end{cases}. \tag{31}$$

Putting (31) into (28) produces

$$\begin{aligned}\dot W|_{(11)}\leq&-2\frac{k_2}{k_1}\alpha_{19}T^{2+\rho}W^{\frac{(1+\rho)(2+\rho)}{2}}\\&+\frac{k_2}{k_1}\alpha_{19}T^{2+\rho}W_{\max}^{\frac{(1+\rho)(2+\rho)}{2}}\\&-2\frac{k_2}{k_1}\alpha_{17}T^{\frac{2+\rho}{1+\rho}}W^{\frac{(1+2\rho)(2+\rho)}{2(1+\rho)}}+\alpha_{17}\frac{k_2}{k_1}T^{\frac{2+\rho}{1+\rho}}W_{\max}^{\frac{(1+2\rho)(2+\rho)}{2(1+\rho)}}.\end{aligned} \tag{32}$$

On the basis of (32), a contradictory argument is used to prove

$$\max_{\forall\gamma\in[t_k,t_{k+1}]}W(\gamma)=W(t_k). \tag{33}$$

It is assumed that (33) is mistaken, which insinuates that there must exist a time instant $t_1\in[t_k,t_{k+1}]$ such that $W(t_1)>W(t_k)$. Since $\dot W(t_k)<0$, there must exist another time instant $t_2\in[t_k,t_1]$ such that: 1) $W(t_2)=W(t_k)$; 2) $W(t)\leq W(t_k)\ \forall t\in[t_k,t_2]$; 3) $\dot W(t_2)>0$. It follows from 1), 2) and (32) that

$$\begin{aligned}\dot W(t_2)\leq&-\frac{k_2}{k_1}\alpha_{19}T^{2+\rho}W^{\frac{(1+\rho)(2+\rho)}{2}}(t_2)\\&-\frac{k_2}{k_1}\alpha_{17}T^{\frac{2+\rho}{1+\rho}}W^{\frac{(1+2\rho)(2+\rho)}{2(1+\rho)}}(t_2)\\<&\,0\end{aligned} \tag{34}$$

which is apparently in contradiction with 3) $\dot W(t_2)>0$. Consequently, (33) is proved. Further, (32) is rewritten as

$$\begin{aligned}\dot W|_{(11)}\leq&-2\frac{k_2}{k_1}\alpha_{19}T^{2+\rho}W^{\frac{(1+\rho)(2+\rho)}{2}}(t)\\&+\frac{k_2}{k_1}\alpha_{19}T^{2+\rho}W^{\frac{(1+\rho)(2+\rho)}{2}}(t_k)\\&-2\frac{k_2}{k_1}\alpha_{17}T^{\frac{2+\rho}{1+\rho}}W^{\frac{(1+2\rho)(2+\rho)}{2(1+\rho)}}(t)\\&+\alpha_{17}\frac{k_2}{k_1}T^{\frac{2+\rho}{1+\rho}}W^{\frac{(1+2\rho)(2+\rho)}{2(1+\rho)}}(t_k).\end{aligned} \tag{35}$$

For $\forall t\in[t_k,t_{k+1})$, there are two cases considered for $W(t)$, including $W(t)>\frac{1}{2}W(t_k)$ and $W(t)\leq\frac{1}{2}W(t_k)$. Manifestly, the case $W(t)>\frac{1}{2}W(t_k)$ always happens. In other words, before $W(t)\leq\frac{1}{2}W(t_k)$, one has

$$\begin{aligned}\dot W|_{(11)}\leq&-\left(2-2^{\frac{(1+\rho)(2+\rho)}{2}}\right)\frac{k_2}{k_1}\alpha_{19}T^{2+\rho}W^{\frac{(1+\rho)(2+\rho)}{2}}(t)\\&-\left(2-2^{\frac{(1+2\rho)(2+\rho)}{2(1+\rho)}}\right)\frac{k_2}{k_1}\alpha_{17}T^{\frac{2+\rho}{1+\rho}}W^{\frac{(1+2\rho)(2+\rho)}{2(1+\rho)}}(t).\end{aligned} \tag{36}$$

Therefore, from (36), regardless of whether the second case $W(t)\leq\frac{1}{2}W(t_k)$ occurs, there is $W(t_{k+1})\leq\varsigma W(t_k)$ with one constant $\varsigma\in(0,1)$. As a result, the system states will finite-time converge to the domain Ψ in (29). Note that from (12) and (29), one has (8). The proof is completed. ■

For the sake of clarity, the block diagram of the proposed controller is shown by Fig. 1.

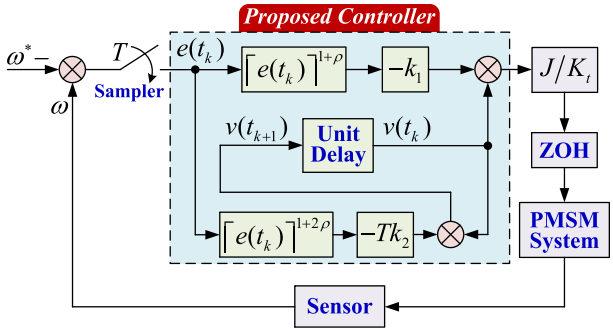

Fig. 1. Block diagram of the presented controller.

Remark 1: It is found that in contrast with the traditional DTST algorithm, the proposed control scheme possesses an additional adjustable parameter ρ, which can play a vital role in making a trade-off between the control energy and the system performance. In addition, note that if the sampling period $T=0$, then the modified discrete-time super-twisting closed-loop system (11) will be reduced to the continuous-time system (13).

Remark 2: It is observed from Theorem 1 that the system output will ultimately converge to a region bounded by $(\frac{D^*}{k_2})^{\frac{1}{1+2\rho}}\sigma_1$ and $T^{-\frac{1}{\rho}}\sigma_2$. The bound $(\frac{D^*}{k_2})^{\frac{1}{1+2\rho}}\sigma_1$ represents the impact on control performance induced by the lumped perturbation. The bound $T^{-\frac{1}{\rho}}\sigma_2$ stands for the chattering influence resulting from the nonsmooth term $\lceil e(t_k)\rfloor^{1+2\rho}$ in (7).

Remark 3: In light of $-\frac{1}{2}<\rho<0$, we will discuss the following two cases. First, if $\rho=-\frac{1}{2}$, controller (7) will become the conventional DTST controller (5). Under such a circumstance, the system output will converge to the region $\{e(t_k):|e(t_k)|\leq T^2\tilde\sigma_2\}$ with one constant $\tilde\sigma_2>0$. One can also see that the lumped perturbation is thoroughly eliminated. Nonetheless, the discontinuity generated from the sign function encompassed in

controller (5) will bring about the unanticipated chattering phenomenon. Second, if $\rho = 0$, controller (7) will be degenerated into the discrete-time linear controller described by

$$\begin{cases} u(t_k) = -k_1 \cdot e(t_k) + v(t_k) \\ v(t_{k+1}) = v(t_k) - Tk_2 \cdot e(t_k) \end{cases} \tag{37}$$

where k_1 and k_2 are suitable positive constants. Under controller (37), the system output will eventually converge to the region $\{e(t_k) : |e(t_k)| \leq \frac{D^*}{k_2}\tilde{\sigma}_1\}$ where $\tilde{\sigma}_1 > 0$ is one constant. In this case, although the chattering effect vanishes, the lumped perturbation will bring the adverse consequence on system performance.

Remark 4: The selection criteria of parameters k_1 and k_2 for controllers (5), (7), and (37) normally rely upon the system characteristics and the conditions of ensuring the system stability. Specifically, k_1 and k_2 in the three controllers evidently impact the convergence speed and robustness of the considered system. The larger k_1 implies the greater control efforts of the three controllers and the faster system responses. Nonetheless, as k_1 is too large, the considered system may oscillate or even become unstable. Moreover, the parameter k_2 can help the three controllers reduce the steady-state errors and make the system output more precise. It is noted that as k_2 is excessively large, the system response speed will slow down, and the windup phenomenon will occur. Hence, we ought to carefully select proper parameters k_1 and k_2 to keep a balance between the robustness and the oscillation in the considered system.

Remark 5: It is indeed true that the performance of the proposed controller is highly dependent on the choice of parameters, which is a common challenge for many control systems. In practice, this issue can be solved through the following three strategies. The first one is the system identification and tuning. This method can be used to accurately model the system dynamics. Further, the obtained model can be utilized to optimize the controller parameters. Such one way ensures that the selected parameters are more aligned with the actual behaviors of systems. The second one is the parameter sensitivity analysis. By conducting such one approach, the relationship between controller parameters and system performances can be well understood. This helps in determining the critical parameters that need to be tuned with the higher precision while providing some robustness against the variations in less critical parameters. The third one is the implementation of several robust control methods in order to mitigate the dependency on exact parameter values. It is seen that these robust control approaches can perform well even in face of the uncertainties or variations in system parameters. This can provide more stability and reliability in real-world applications where the exact parameter values may be difficult to maintain.

IV. Experimental Results

In the section, the presented control strategy will be experimentally verified. The experimental configuration and its setup are respectively depicted by Figs. 2–3. Such a setup mainly comprises the computer with MATLAB/Simulink (Intel Core I5 11400), the real-time digital controller RTU-BOX204, the three-phase inverter RTM-PEF4035IF, the dc power supply

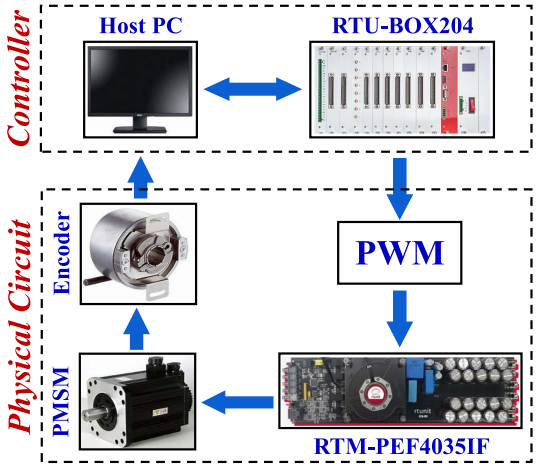

Fig. 2. Configuration of experimental system.

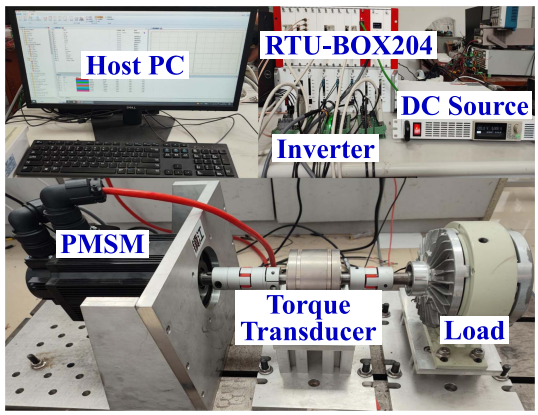

Fig. 3. Setup of experimental system.

RTP-DSL30010, the torque transducer, the magnetic powder brake, the incremental encoder with 2500 lines, and the surface-mounted PMSM. The field oriented control is adopted in the PMSM drive system for all the control strategies to make a fair assessment. The general specifications of PMSM are listed in Table I.

A. Comparative Results Among Different Controllers

In order to confirm the merit of the proposed modified DTST controller (7), the discrete-time linear controller (37) and the conventional DTST controller (5) are utilized for the control performance comparisons and evaluations in the experiment. The reference velocity ω^* is 500 r/min. All the controllers are configured to attain the optimal performance in terms of the tracking precision and the convergence speed. Specifically, the parameters of controllers (5) and (37) are set as $k_1 = 1.8$, $k_2 = 21.4$, and $T = 0.001$ s, while the parameters of controller (7) are configured as $\rho = -0.2$, $k_1 = 1.8$, $k_2 = 21.4$, and $T = 0.001$ s. The corresponding results are exhibited in Figs. 4–5.

Fig. 4 depicts the step speed response curves without the load. Concentrating on this figure, we can observe that the speed overshoot under the presented controller (7) is smaller than that

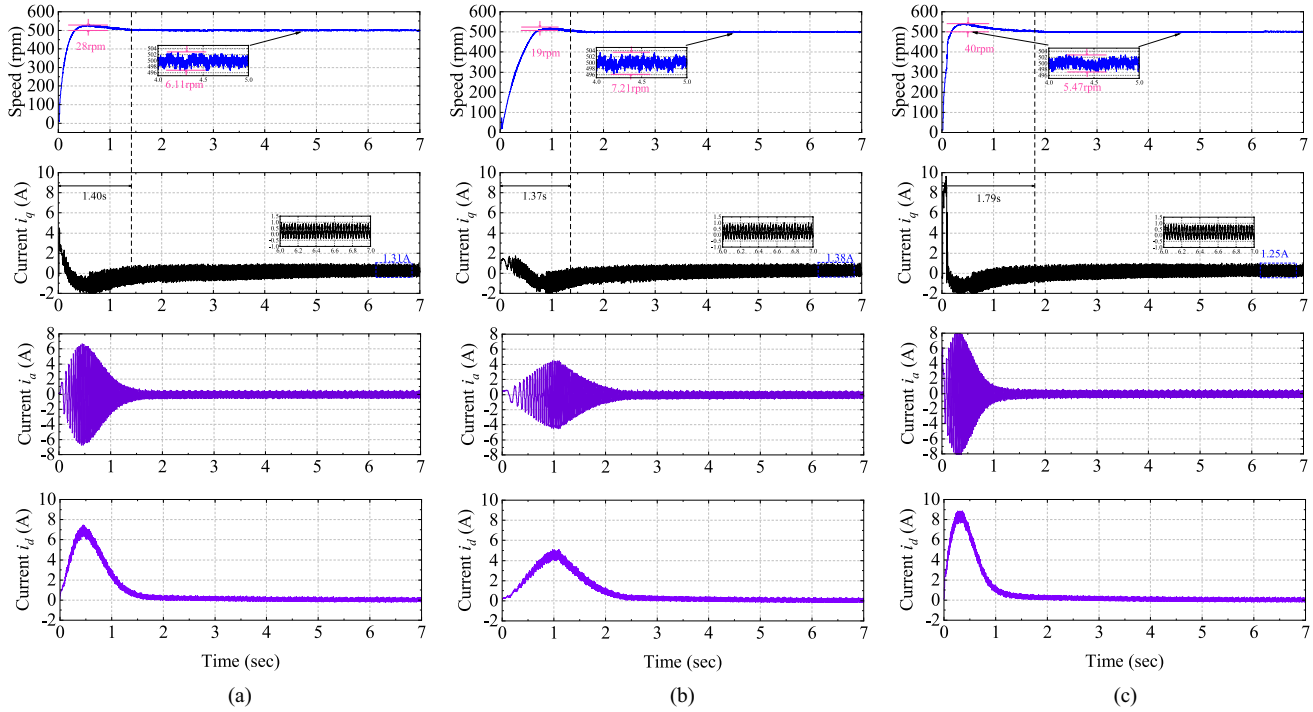

Fig. 4. Step responses under three controllers without load. (a) Controller (7). (b) Controller (5). (c) Controller (37).

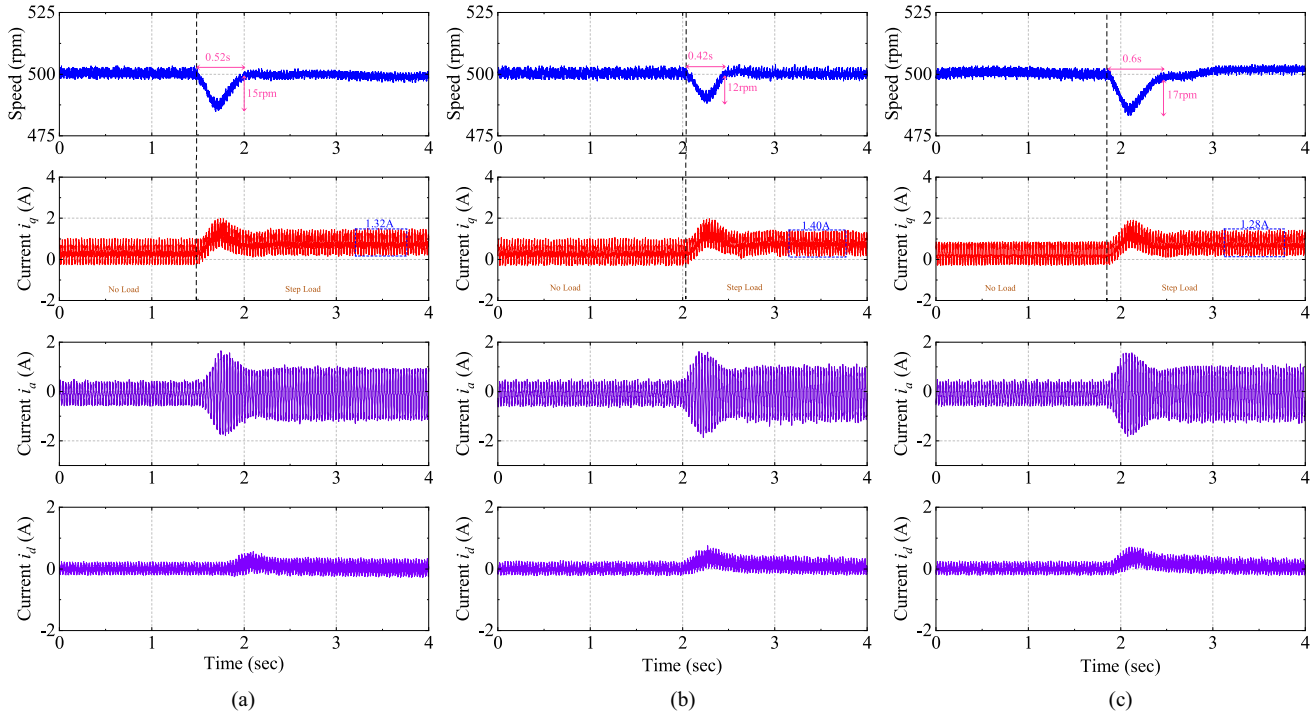

Fig. 5. Responses under three controllers with sudden load torque variations. (a) Controller (7). (b) Controller (5). (c) Controller (37).

under controller (37) but bigger than that under controller (5) at the no-load start-up phase. In addition, the ripple of the q-axis current under controller (7) is smaller than that under controller (5) but larger than that under controller (37) after the speed response enters into the steady state.

Fig. 5 shows how the speed and the q-axis current respond to the sudden load torque variations at a constant speed of 500 r/min. By observing this figure, it is clear that under controller (7), the recovery time is 0.52 s, which is shorter than that under controller (37). Besides, the speed drop under controller

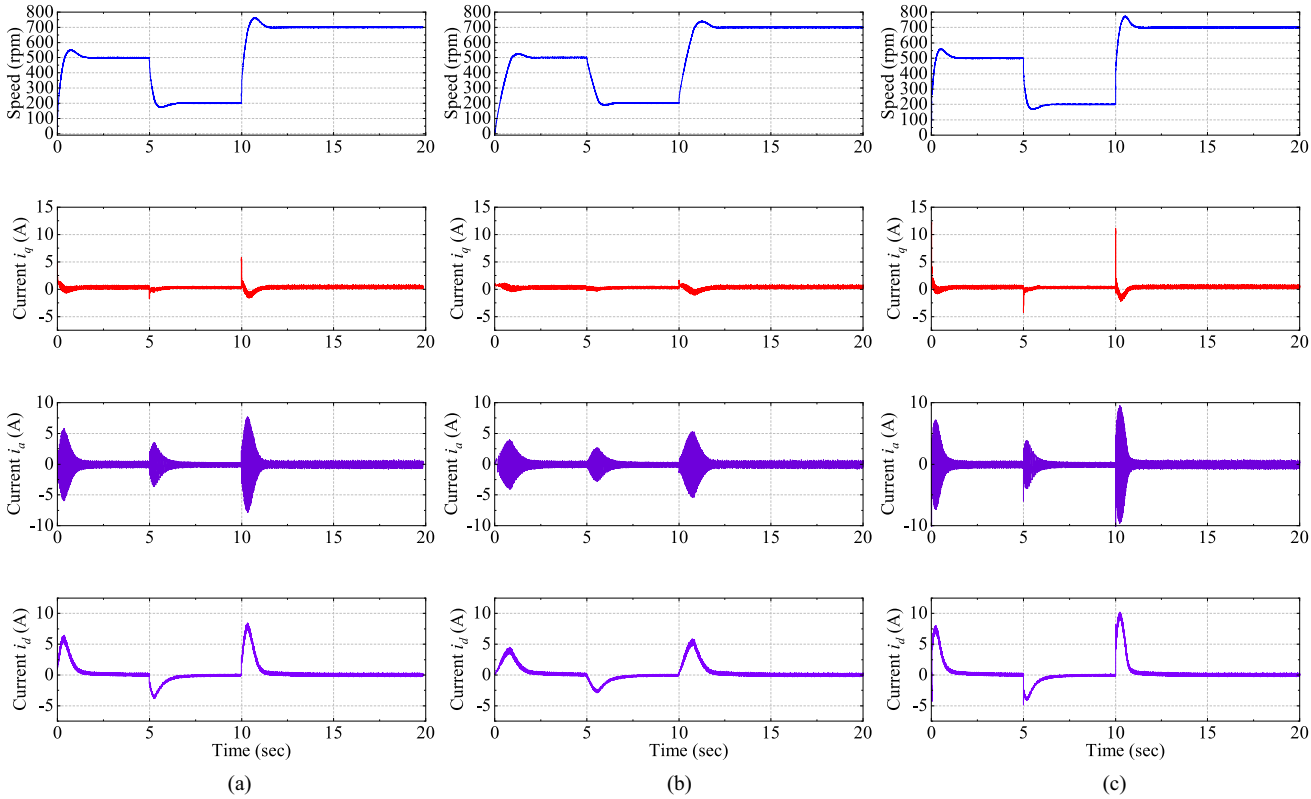

Fig. 6. Sudden speed change responses under three controllers without load. (a) Controller (7). (b) Controller (5). (c) Controller (37).

TABLE I
NOMINAL PARAMETERS OF EXPERIMENTAL PMSM

Symbol	Implication	Value	Unit
I_n	Rated current	6	A
U_n	Rated voltage	220	V
P_r	Rated power	1.5	kW
N_n	Rated speed	1500	r/min
T_n	Rated torque	10	N·m
P_n	Number of pole pairs	4	–
R_s	Stator resistance	1.5	Ω
L_s	Stator inductance	4.37	mH
ψ_f	Flux linkage	0.142	Wb
J	Moment of inertia	1.94×10^{-3}	kg·m^2
M	Motor mass	10.2	kg

TABLE II
QUANTITATIVE COMPARISON OF CONTROL PERFORMANCES WITHOUT LOAD

Controller	(7)	(5)	(37)
Overshoot (%)	5.6	3.8	8
Settling Time (s)	1.40	1.37	1.79
Speed Fluctuation (rpm)	6.11	7.21	5.47

TABLE III
QUANTITATIVE COMPARISON OF CONTROL PERFORMANCES WITH SUDDEN LOAD TORQUE VARIATIONS

Controller	(7)	(5)	(37)
Maximum Speed Decrease (rpm)	15	12	17
Recovery Time (s)	0.52	0.42	0.6
Current Ripple (A)	1.32	1.40	1.28

(37) is 17 r/min, which is largest among the three controllers. It insinuates that the discrete-time linear controller (37) possesses the weakest disturbance rejection ability.

In order to further assess the performances under the three control schemes, the quantitative comparisons without load and with sudden load torque variations are, respectively, listed in Tables II and III. It can be found that the speed fluctuation and the current ripple under controller (7) are smaller than those under controller (5).

In summary, in view of the aforesaid experimental results, when simultaneously considering the current ripple and the robustness performance, the suggested controller (7) is superior to controllers (5) and (37).

Moreover, the results of a sudden speed change are given to test the robustness of the three controllers, as shown in Fig. 6. One can observe from this figure that under the three controllers, the starting speed is 500 r/min. At the fifth second, the speed decreases to 200 r/min. At the tenth second, the speed increases

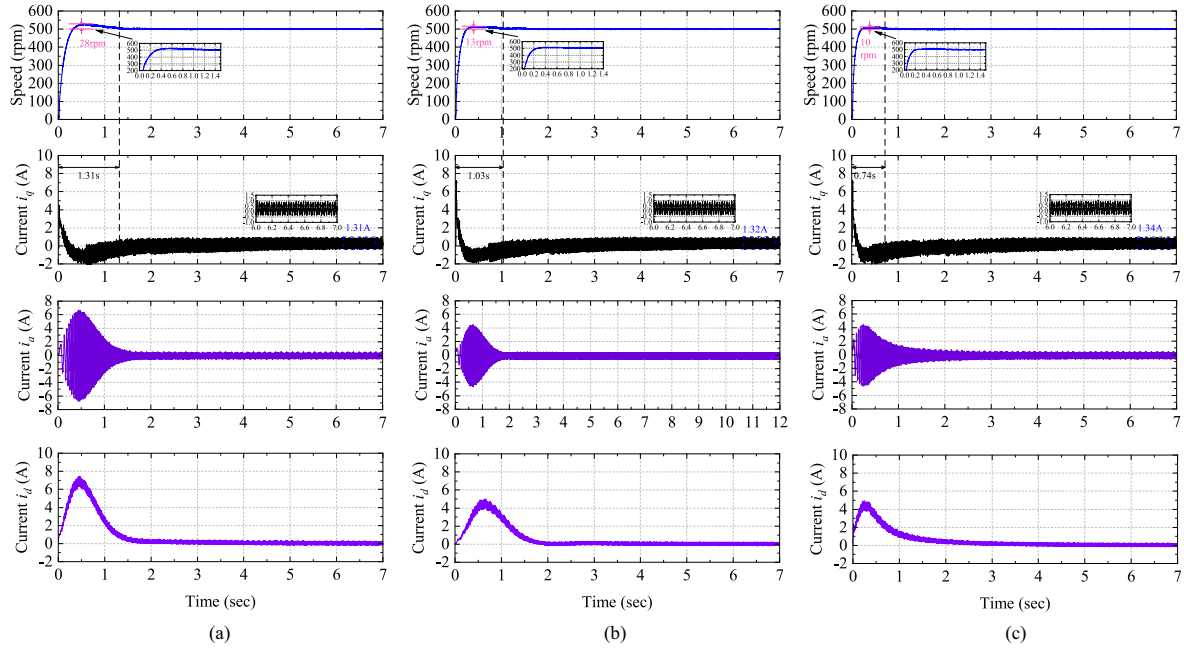

Fig. 7. Step responses of different values for parameter k_1 without load. (a) $k_1 = 1.8$. (b) $k_1 = 2.8$. (c) $k_1 = 3.8$.

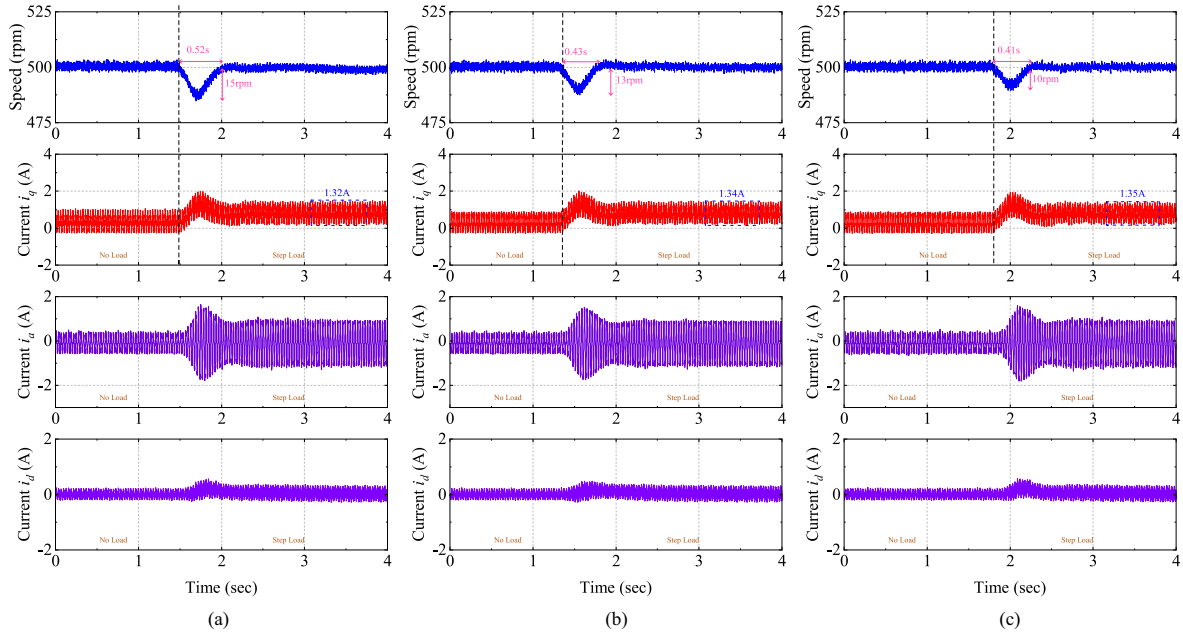

Fig. 8. Responses of different values for parameter k_1 under sudden load torque variations. (a) $k_1 = 1.8$. (b) $k_1 = 2.8$. (c) $k_1 = 3.8$.

to 700 r/min. Therefore, the robustness of the controllers related to a sudden speed change is presented.

B. Impact of Modified DTST Controller Parameters

Under the scenario, several experiments are implemented to respectively explore and discuss how k_1, ρ, and T of controller (7) influence the performance of the PMSM system. To be specific, we study the following three different cases.

Case 1 (For Different Values of Parameter k_1): The parameter k_1 is respectively set as $k_1 = 1.8, 2.8, 3.8$. Let $\rho = -0.2$ and $k_2 = 21.4$. The derived experiment results are shown by Figs. 7–8.

It is clear to see from Fig. 7 that under the developed controller (7), the larger value of k_1 signifies the smaller speed overshoot and the shorter settling time without the extra load torque during the starting procedure, thereby enhancing the startup dynamic performance of the PMSM system. Nevertheless, increasing k_1

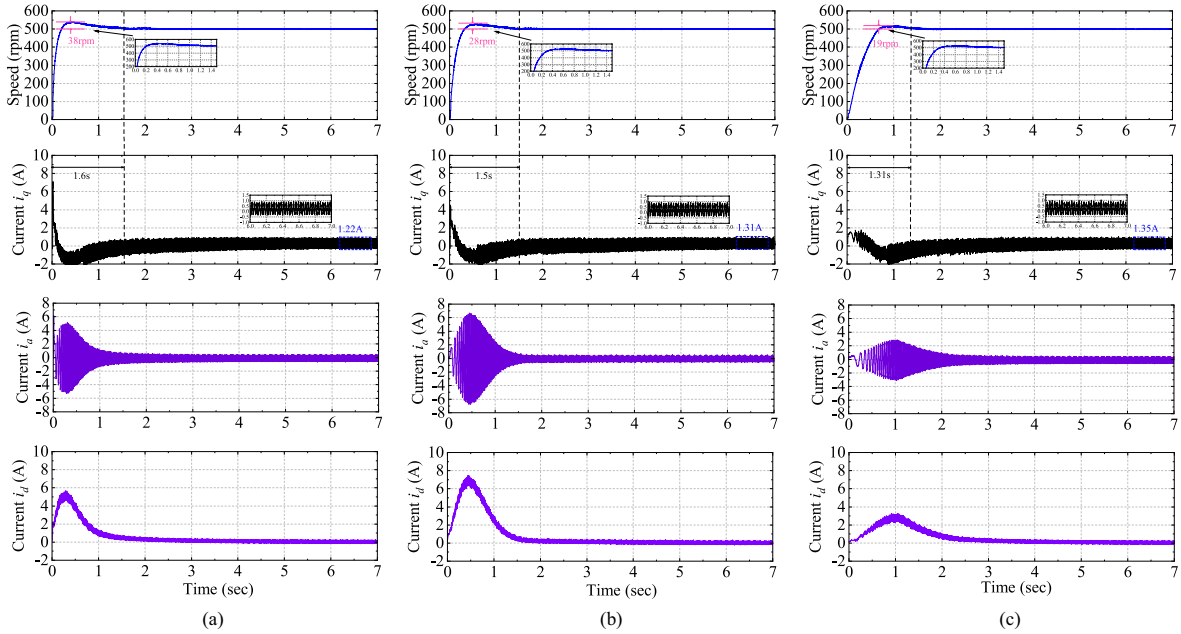

Fig. 9. Step responses of different values for parameter ρ without load. (a) $\rho = -0.01$. (b) $\rho = -0.2$. (c) $\rho = -0.49$.

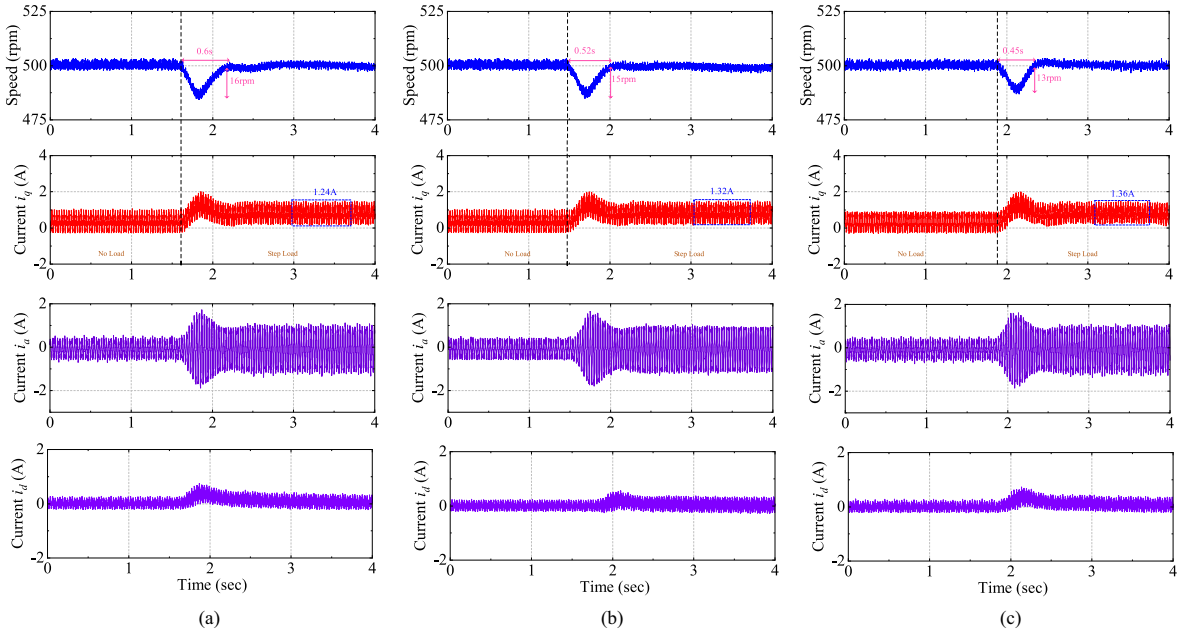

Fig. 10. Responses of different values for parameter ρ under sudden load torque variations. (a) $\rho = -0.01$. (b) $\rho = -0.2$. (c) $\rho = -0.49$.

will bring about the relative enlargement for the fluctuation of the q-axis current. In addition, Fig. 8 is given to test the relation between the antiinterference performance of PMSM and the parameter k_1. It can be found that the bigger k_1 gives rise to the shorter recovery time and the smaller speed drop in the case of sudden load increase imposed on the PMSM as the reference velocity is 500 rpm. In other words, increasing k_1 insinuates the stronger robustness of PMSM. However, the larger k_1 will ineluctably result in the increase of the q-axis current fluctuation. Consequently, the parameter k_1 should be suitably chosen to maintain a balance between the desirable robustness and the current ripple.

Case 2 (For Different Values of Parameter ρ): We select the parameter ρ as $-0.49, -0.2, -0.01$, respectively. Let $k_1 = 1.8$ and $k_2 = 21.4$. Figs. 9–10 display the obtained experimental results.

The step response curves of speed and i_q current in the absence of the load torque with $\rho = -0.49, -0.2, -0.01$ are exhibited

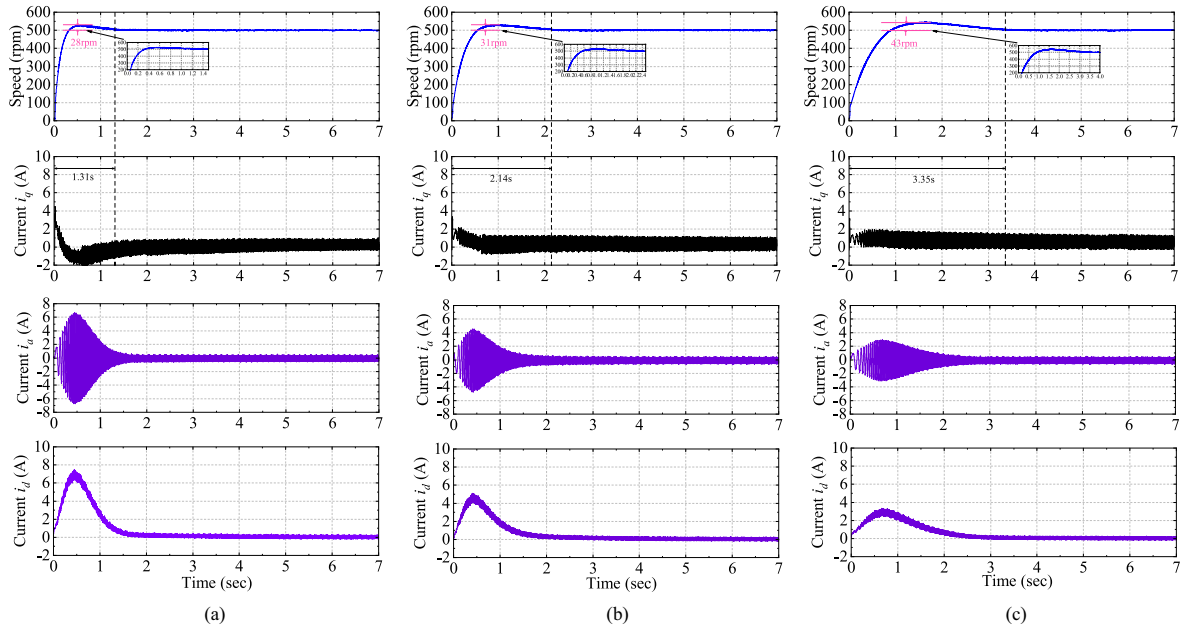

Fig. 11. Step responses of different sampling periods without load. (a) $T = 1$ ms. (b) $T = 0.5$ ms. (c) $T = 0.25$ ms.

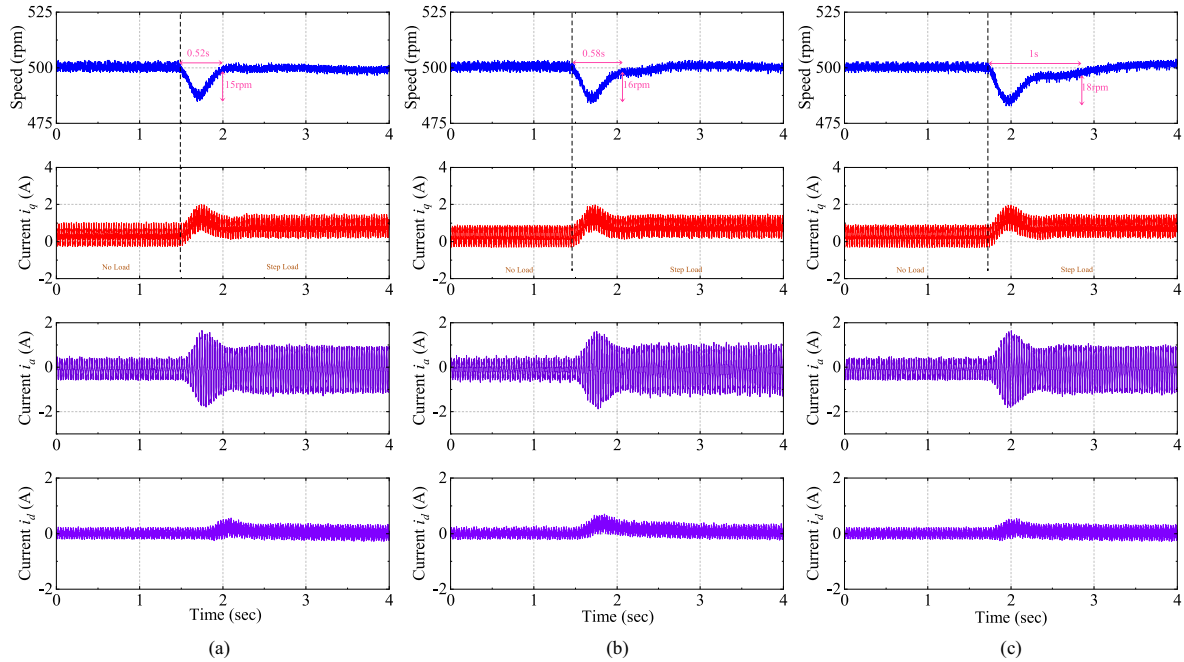

Fig. 12. Responses of different sampling periods under sudden load torque variations. (a) $T = 1$ ms. (b) $T = 0.5$ ms. (c) $T = 0.25$ ms.

in Fig. 9. From this figure, we can clearly find that along with the reduction of the parameter ρ, the speed overshoot and the recovery time decrease. Nonetheless, there is a corresponding increase in the current ripple as the parameter ρ decreases within the interval $(-0.5, 0)$. Moreover, Fig. 10 depicts the response curves of different values for parameter ρ under a sudden load change. It can be evidently observed that when the parameter ρ is, respectively, chosen as $-0.49, -0.2, -0.01$, the corresponding speed drop is, respectively, $13, 15, 16$ r/min, and the corresponding recovery time is respectively $0.45, 0.52, 0.6$ s. This indicates that the smaller ρ in the range $(-0.5, 0)$ leads to the larger current fluctuation and the stronger antidisturbance ability of PMSM.

Case 3 (For Different Values of Sampling Period T): Herein, the performance of controller (7) for system (4) will be investigated under different sampling periods. Let $k_1 = 1.8$, $k_2 = 21.4$ and $\rho = -0.2$. We choose the sampling period T as 1 ms, 0.5 ms,

TABLE IV
QUANTITATIVE INDEXES OF SPEED TRACKING PERFORMANCES

Sampling period	MAE	IAE
1 ms	1.1059	2.7648
0.5 ms	1.0455	2.6138
0.25 ms	1.0397	2.5993

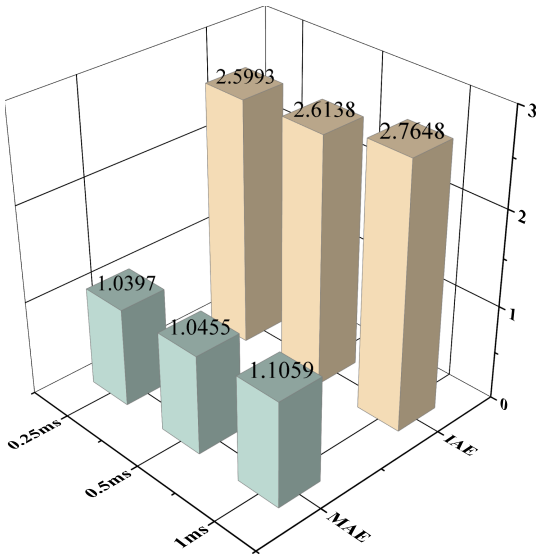

Fig. 13. Comparisons of quantitative indexes under different sampling periods.

and 0.25 ms, respectively. The acquired experiment results are displayed through Figs. 11–12.

From Figs. 11–12, we can obviously observe that when the sampling period is increased, both the response speed and the antidisturbance capability of PMSM are improved. In order to qualitatively evaluate the control performance, the mean absolute error (MAE) $\frac{1}{N}\sum_{i=1}^{N}|e(i)|$ and the integral absolute error (IAE) $\sum_{i=0}^{N}(|e(i)|\Delta t)$ are chosen as quantitative indexes. As shown in Table IV and Fig. 13, the smaller sampling period implies the smaller MAE and IAE, thereby indicating the higher control precision.

V. CONCLUSION

In our work, a modified DTST control approach to the speed regulation system of PMSM is devised. In comparison with the discrete-time linear controller and the conventional DTST, the presented strategy is capable of attaining the higher control precision and the stronger robustness with attenuating the chattering impact during the digital execution. It is achieved mainly due to the utilization of the nonsmooth term, which can generate an extra fractional power parameter to flexibly adjust the system control performances. The closed-loop convergence analysis are rigorously validated through the theoretically comprehensive investigation. The substantial comparative hardware experiment studies are performed to substantiate the reliability and advantage of the presented strategy. The future research will be committed to addressing the sensorless speed regulation issue for PMSM under the proposed approach.

APPENDIX
IMPORTANT LEMMAS

Lemma 1 ([46]): For any $\theta > 0$, one has for $\forall x, y \in \mathbb{R}$, $(|x| + |y|)^{\theta} \le \max\{1, 2^{\theta-1}\}(|x|^{\theta} + |y|^{\theta})$.

Lemma 2 ([47]): Let $\varphi(x_1, x_2) > 0$ be a function of x_1 and x_2 for $\forall x_1, x_2 \in \mathbb{R}$. For any $c_1, c_2 > 0$, there is $|x_1|^{c_1}|x_2|^{c_2} \le \frac{c_1}{c_1+c_2}\varphi(x_1, x_2)|x_1|^{c_1+c_2} + \frac{c_2}{c_1+c_2}(\varphi(x_1, x_2))^{-\frac{c_1}{c_2}}|x_2|^{c_1+c_2}$.

Lemma 3 ([46]): If $0 < b \le 1$, for $\forall x, y \in \mathbb{R}$, there is $|\lceil x \rceil^{b} - \lceil y \rceil^{b}| \le 2^{1-b}|x - y|^{b}$.

REFERENCES

[1] X. Lin et al., "Observer-based fixed-time control for permanent-magnet synchronous motors with parameter uncertainties," *IEEE Trans. Power Electron.*, vol. 38, no. 4, pp. 4335–4344, Apr. 2023.
[2] M. Hu, W. Hua, Z. Wang, S. Li, P. Wang, and Y. Wang, "Selective periodic disturbance elimination using extended harmonic state observer for smooth speed control in PMSM drives," *IEEE Trans. Power Electron.*, vol. 37, no. 11, pp. 13288–13298, Nov. 2022.
[3] K. Shao, J. Zheng, R. Tang, X. Li, Z. Man, and B. Liang, "Barrier function based adaptive sliding mode control for uncertain systems with input saturation," *IEEE/ASME Trans. Mechatron.*, vol. 27, no. 6, pp. 4258–4268, Dec. 2022.
[4] J. Yang, W.-H. Chen, S. Li, L. Guo, and Y. Yan, "Disturbance/uncertainty estimation and attenuation techniques in PMSM drives—A survey," *IEEE Trans. Ind. Electron.*, vol. 64, no. 4, pp. 3273–3285, Apr. 2017.
[5] L. Zhang and J. Fei, "Intelligent complementary terminal sliding mode using multiloop neural network for active power filter," *IEEE Trans. Power Electron.*, vol. 38, no. 8, pp. 9367–9383, Aug. 2023.
[6] Z. Yang, C. Qian, X. Sun, and K. Wang, "Enhanced linear ADRC strategy for sensorless control of IPMSM considering cross-coupling factors," *IEEE Trans. Transport. Electrific.*, vol. 9, no. 3, pp. 4437–4446, Sep. 2023.
[7] W. Qian, S. K. Panda, and J.-X. Xu, "Torque ripple minimization in PM synchronous motors using iterative learning control," *IEEE Trans. Power Electron.*, vol. 19, no. 2, pp. 272–279, Mar. 2004.
[8] W. Dou, S. Ding, J. H. Park, and K. Mei, "An adaptive generalized super-twisting algorithm via event-triggered control," *IEEE Trans. Automat. Sci. Eng.*, vol. 22, pp. 393–406, 2025.
[9] Y.-S. Kung and M.-H. Tsai, "FPGA-based speed control IC for PMSM drive with adaptive fuzzy control," *IEEE Trans. Power Electron.*, vol. 22, no. 6, pp. 2476–2486, Nov. 2007.
[10] S. Li, K. Zong, and H. Liu, "A composite speed controller based on a second-order model of permanent magnet synchronous motor system," *Trans. Inst. Meas. Control*, vol. 33, no. 5, pp. 522–541, Jul. 2011.
[11] Y. Feng, X. Yu, and Z. Man, "Non-singular terminal sliding mode control of rigid manipulators," *Automatica*, vol. 38, no. 12, pp. 2159–2167, Dec. 2002.
[12] S. Li, M. Zhou, and X. Yu, "Design and implementation of terminal sliding mode control method for PMSM speed regulation system," *IEEE Trans. Ind. Informat.*, vol. 9, no. 4, pp. 1879–1891, Nov. 2013.
[13] B. Xu, L. Zhang, and W. Ji, "Improved non-singular fast terminal sliding mode control with disturbance observer for PMSM drives," *IEEE Trans. Transp. Electrific.*, vol. 7, no. 4, pp. 2753–2762, Dec. 2021.
[14] W. Dou, S. Ding, and J. H. Park, "Practical event-triggered finite-time second-order sliding mode controller design," *IEEE Trans. Cybern.*, vol. 54, no. 3, pp. 1972–1983, Mar. 2024.
[15] J. Sun, Q. Li, S. Ding, G. Xing, and L. Chen, "Fixed-time generalized super-twisting control for path tracking of autonomous agricultural vehicles considering wheel slipping," *Comput. Electron. Agriculture*, vol. 213, Oct. 2023, Art. no. 108231.
[16] L. Chen, H. Zhang, H. Wang, K. Shao, G. Wang, and A. Yazdani, "Continuous adaptive fast terminal sliding mode-based speed regulation control of PMSM drive via improved super-twisting observer," *IEEE Trans. Ind. Electron.*, vol. 71, no. 5, pp. 5105–5115, May 2024.

[17] I. Boiko, L. Fridman, A. Pisano, and E. Usai, "Analysis of chattering in systems with second-order sliding modes," *IEEE Trans. Autom. Control*, vol. 52, no. 11, pp. 2085–2102, Nov. 2007.
[18] S. V. Emelyanov, S. K. Korovin, and L. V. Levantovsky, "Second order sliding modes in controlling uncertain systems," *Sov. J. Comput. Syst. Sci.*, vol. 24, no. 4, pp. 63–68, Jul. 1986.
[19] H. Haimovich, L. Fridman, and J. A. Moreno, "Generalized super-twisting for control under time- and state-dependent perturbations: Breaking the algebraic loop," *IEEE Trans. Autom. Control*, vol. 67, no. 10, pp. 5646–5652, Oct. 2022.
[20] S. Kamal, J. A. Moreno, A. Chalanga, B. Bandyopadhyay, and L. Fridman, "Continuous terminal sliding-mode controller," *Automatica*, vol. 69, pp. 308–314, Jul. 2016.
[21] R. Seeber, M. Reichhartinger, and M. Horn, "A Lyapunov function for an extended super-twisting algorithm," *IEEE Trans. Autom. Control*, vol. 63, no. 10, pp. 3426–3433, Oct. 2018.
[22] Q. Hou, S. Ding, and X. Yu, "Composite super-twisting sliding mode control design for PMSM speed regulation problem based on a novel disturbance observer," *IEEE Trans. Energy Convers.*, vol. 36, no. 4, pp. 2591–2599, Dec. 2021.
[23] L. Chen et al., "Sensorless fixed-time sliding mode control of PMSM based on barrier function adaptive super-twisting observer," *IEEE Trans. Power Electron.*, vol. 39, no. 3, pp. 3037–3051, Mar. 2024.
[24] C. Ding, S. Ding, X. Wei, X. Ji, J. Sun, and K. Mei, "Disturbance-observer-based barrier function adaptive sliding mode control for path tracking of autonomous agricultural vehicles with matched-mismatched disturbances," *IEEE Trans. Transp. Electrific.*, vol. 10, no. 3, pp. 6748–6760, Sep. 2024.
[25] Q. Hou and S. Ding, "Finite-time extended state observer-based super-twisting sliding mode controller for PMSM drives with inertia identification," *IEEE Trans. Transp. Electrific.*, vol. 8, no. 2, pp. 1918–1929, Jun. 2022.
[26] Z. Galias and X. Yu, "Euler's discretization of single input sliding-mode control systems," *IEEE Trans. Autom. Control*, vol. 52, no. 9, pp. 1726–1730, Sep. 2007.
[27] X. Yu, B. Wang, Z. Galias, and G. Chen, "Discretization effect on equivalent control-based multi-input sliding-mode control systems," *IEEE Trans. Autom. Control*, vol. 53, no. 6, pp. 1563–1569, Jul. 2008.
[28] S. Qu, X. Xia, and J. Zhang, "Dynamical behaviors of an euler discretized sliding mode control systems," *IEEE Trans. Autom. Control*, vol. 59, no. 9, pp. 2525–2529, Sep. 2014.
[29] W. Gao, Y. Wang, and A. Homaifa, "Discrete-time variable structure control systems," *IEEE Trans. Ind. Electron.*, vol. 42, no. 2, pp. 117–122, Apr. 1995.
[30] S. Qu, X. Xia, and J. Zhang, "Dynamics of discrete-time sliding-mode-control uncertain systems with a disturbance compensator," *IEEE Trans. Ind. Electron.*, vol. 61, no. 7, pp. 3502–3510, Jul. 2014.
[31] J. Zhang, P. Shi, Y. Xia, and H. Yang, "Discrete-time sliding mode control with disturbance rejection," *IEEE Trans. Ind. Electron.*, vol. 66, no. 10, pp. 7967–7975, Oct. 2019.
[32] A. K. Behera and B. Bandyopadhyay, "Steady-state behaviour of discretized terminal sliding mode," *Automatica*, vol. 54, pp. 176–181, Apr. 2015.
[33] H. Du, X. Yu, M. Z. Q. Chen, and S. Li, "Chattering-free discrete-time sliding mode control," *Automatica*, vol. 68, pp. 87–91, Jun. 2016.
[34] K. Abidi, J.-X. Xu, and J.-H. She, "A discrete-time terminal sliding-mode control approach applied to a motion control problem," *IEEE Trans. Ind. Electron.*, vol. 56, no. 9, pp. 3619–3627, Sep. 2009.
[35] H. Du, G. Wen, Y. Cheng, W. Lu, and T. Huang, "Designing discrete-time sliding mode controller with mismatched disturbances compensation," *IEEE Trans. Ind. Informat.*, vol. 16, no. 6, pp. 4109–4118, Jun. 2020.
[36] V. Repecho, D. Biel, and A. Arias, "Fixed switching period discrete-time sliding mode current control of a PMSM," *IEEE Trans. Ind. Electron.*, vol. 65, no. 3, pp. 2039–2048, Mar. 2018.
[37] Y. Yan, Z. Galias, X. Yu, and C. Sun, "Euler's discretization effect on a twisting algorithm based sliding mode control," *Automatica*, vol. 68, pp. 203–208, Jun. 2016.
[38] S. Koch and M. Reichhartinger, "Discrete-time equivalents of the super-twisting algorithm," *Automatica*, vol. 107, pp. 190–199, Sep. 2019.
[39] B. Brogliato, A. Polyakov, and D. Efimov, "The implicit discretization of the supertwisting sliding-mode control algorithm," *IEEE Trans. Autom. Control*, vol. 65, no. 8, pp. 3707–3713, Aug. 2020.
[40] Y. Yan, S. Yu, and X. Yu, "Euler's discretization effect on a sliding-mode control system with supertwisting algorithm," *IEEE Trans. Autom. Control*, vol. 66, no. 6, pp. 2817–2824, Jun. 2021.
[41] Y. Zuo, X. Zhu, L. Quan, C. Zhang, Y. Du, and Z. Xiang, "Active disturbance rejection controller for speed control of electrical drives using phase-locking loop observer," *IEEE Trans. Ind. Electron.*, vol. 66, no. 3, pp. 1748–1759, Mar. 2019.
[42] L. Zhang, Z. Chen, X. Yu, Y. Yang, and S. Li, "Sliding-mode-based robust output regulation and its application in PMSM servo systems," *IEEE Trans. Ind. Electron.*, vol. 70, no. 2, pp. 1852–1860, Feb. 2023.
[43] W. Yang, S. Ding, and C. Ding, "Fast supertwisting sliding mode control with antipeaking extended state observer for path-tracking of unmanned agricultural vehicles," *IEEE Trans. Ind. Electron.*, vol. 71, no. 10, pp. 12973–12982, Oct. 2024.
[44] W. Chen and H. Du, "A second-order discrete-time super-twisting control algorithm based on homogeneous system theory," *Control Theory Appl.*, vol. 39, no. 4, pp. 761–769, Apr. 2022.
[45] H. Du, C. Qian, S. Yang, and S. Li, "Recursive design of finite-time convergent observers for a class of time-varying nonlinear systems," *Automatica*, vol. 49, no. 2, pp. 601–609, Feb. 2013.
[46] K. Mei, S. Ding, X. Dai, and C.-C. Chen, "Design of second-order sliding-mode controller via output feedback," *IEEE Trans. Syst., Man, Cybern., Syst.*, vol. 54, no. 7, pp. 4371–4380, Jul. 2024.
[47] C. Qian and J. Li, "Global output feedback stabilization of upper-triangular nonlinear systems using a homogeneous domination approach," *Int. J. Robust Nonlinear Control*, vol. 16, no. 9, pp. 441–463, Jun. 2006.

Keqi Mei (Member, IEEE) was born in Jiangsu, China. He received the Ph.D. degree in control science and engineering from Jiangsu University, Zhenjiang, China, in 2021.

From 2019 to 2020, he visited the Department of Electrical and Computer Engineering, The University of Texas at San Antonio, San Antonio, TX, USA. Since 2022, he has been with the School of Electrical and Information Engineering, Jiangsu University. His research interests include constrained control, sliding mode control, and their applications.

Qiyue Li was born in Jiangsu, China, in 1998. He is currently working toward the M.S. degree in control engineering with the School of Electrical and Information Engineering, Jiangsu University, Zhenjiang, China.

His current research interests include nonlinear control and its applications to permanent magnet synchronous motor servo systems and unmanned agricultural machinery.

Weile Chen received the B.E. and M.E. degrees in automatic control from the Hefei University of Technology, Hefei, China, in 2019 and 2022, respectively. He is currently working toward the Ph.D. degree in automatic control with Southeast University, Nanjing, China.

His current research interests include nonsmooth control theory, sliding-mode control theory, and multiagent systems.

Chih-Chiang Chen (Senior Member, IEEE) received the Ph.D. degree in control theory from National Chiao Tung University, Hsinchu, Taiwan, in 2017.

From 2015 to 2016, he was a Visiting Scholar with the Department of Electrical and Computer Engineering, University of Texas at San Antonio, TX, USA. Since 2017, he has been with the Department of Systems and Naval Mechatronic Engineering, National Cheng Kung University, Tainan City, Taiwan, where he is currently an Associate Professor. His research interests include nonlinear systems, nonsmooth control, and homogeneous system theory.

Dr. Chen currently serves as an Associate Editor for *Journal of The Franklin Institute*, *Franklin Open*, *IET Control Theory & Applications*, *International Journal of Control, Automation, and Systems*, *Asian Journal of Control*, and *International Journal of Fuzzy Systems*. He also works as a Subject Editor for *Nonlinear Dynamics* and *International Journal of Robust and Nonlinear Control*.

Shihong Ding (Senior Member, IEEE) was born in Anhui, China. He received the B.E. degree in mathematics from Anhui Normal University, Wuhu, China, in 2004, and the M.S. and Ph.D. degrees in automatic control from Southeast University, Nanjing, China, in 2007 and 2010, respectively.

From 2008 to 2009, he visited The University of Texas at San Antonio, TX, USA. After graduation, he held a research fellowship with the University of Western Sydney, Penrith, Australia, for one year. In 2018, he visited Yeungnam University, South Korea, and from 2019 to 2020, with RMIT University, Melbourne, Australia. Since 2010, he has been with the School of Electrical and Information Engineering, Jiangsu University, Zhenjiang, China, where he is currently a Full Professor. His research interests include sliding mode control and finite-time stability.

Dr. Ding also serves as a Subject Editor/Associate Editor for IEEE TRANSACTIONS ON INDUSTRIAL ELECTRONICS, *Nonlinear Dynamics*, and *International Journal of Adaptive Control and Signal Processing*.